Polymer Capsules

DOI: 10.1002/anie.201302092

Preparation of Nano- and Microcapsules by Electrophoretic Polymer Assembly**

*Joseph J. Richardson, Hirotaka Ejima, Samuel L. Lörcher, Kang Liang, Philipp Senn, Jiwei Cui, and Frank Caruso**

Nano- and microcapsules are of significant interest for application in biomedicine, especially in diagnostics and therapeutic delivery.[1] The fabrication of polymer capsules is often accomplished by the particle-mediated assembly of polymer films, whereby films are formed on particles through polymerization[1a,2] or by depositing multiple polymer layers through layer-by-layer (LbL) assembly.[3] In particular, LbL assembly enables the use of particles of various types, shapes, and sizes as templates and enables a suite of polymers with different properties (functionality, responsiveness, and degradability) to be used to engineer the physical, chemical, and biological properties of the capsules.[4] The versatility of LbL assembly with particle templates has led to the development of a range of coated particles and capsules for diverse applications, including drug and vaccine delivery.[1d–f,4a–f]

Despite the significant progress in the field of LbL-engineered particles, the film-deposition process typically requires numerous centrifugation and rinse steps to separate the coating material (e.g., polymer) and the particles. Furthermore, it is generally limited to particles either dense and/or large enough for centrifugal sedimentation.[4] Other methods to generate LbL capsules have also been reported: for example, atomization techniques,[5] filter membranes,[6] and microfluidic systems[7] have been used; however, each of these approaches reduces the diversity of the types of particles and polymers that can be employed. These limitations highlight the necessity for the development of alternative rapid and robust approaches for the formation of LbL-assembled coatings on particles to generate engineered core–shell particles and capsules.

Herein, we report an electrophoretic polymer assembly (EPA) technique for depositing a range of polymers on particles of different sizes. In this approach, electrophoresis is used to generate particles coated with multiple polymer layers and, following core removal, polymer multilayer capsules. An inherent requirement of EPA is the immobilization of particles in a porous hydrogel; in this study, namely, the biologically derived polysaccharide agarose. Agarose has historically been used with electrophoresis to separate biopolymers (e.g., proteins and nucleic acids) because it gelates under ambient conditions, shows low reactivity, is easy to prepare, and has various, tunable pore sizes.[8] In the present system, agarose acts as a "natural immobilizing microfluidic system". However, we did not use electrophoresis to simply separate free polymer from deposited polymer, but also to deposit the polymers on immobilized particles (Figure 1). This technique reduces handling times, minimizes the potential for aggregation (especially for smaller particles), and opens up the possibility of automating particle-based LbL assembly. Importantly, no novel apparatus is needed, and standard electrophoresis buffers used typically for DNA and RNA separation[9] are used as conductive media to carry the electric charge and polymers through the agarose.

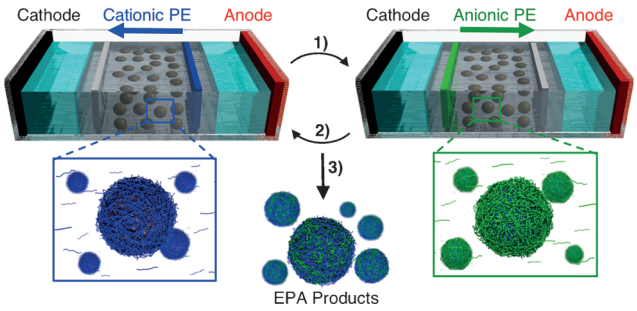

Figure 1. The EPA process for LbL polymer deposition on particles. 1) A cationic polyelectrolyte (PE) is loaded into the wells adjacent to the anode and electrophoresed; it coats the particles as it moves toward the cathode. 2) An anionic PE is loaded into the wells adjacent to the cathode and electrophoresed; it coats the cationic PE-coated particles as it moves toward the anode. Steps 1 and 2 are repeated until the desired number of bilayers have been formed. 3) The agarose is heated, and the EPA products (polymer-coated particles) are recovered.

As a first example, silica (SiO_2) particles with a diameter of 3.08 μm were immobilized in agarose and subjected to EPA with the widely used LbL polyelectrolytes poly(allylamine hydrochloride) (PAH) and poly(styrene sulfonate) (PSS). Approximately 85% of the immobilized particles were recovered, as assessed by flow cytometry: an amount comparable to template recovery in conventional LbL assembly.[4g] Upon core removal, robust capsules were produced that retained the fluorescence of the constituent polymers. The capsules could be centrifuged and washed into different buffers. Although, in this case, the capsules were obtained from the coated particles prepared by EPA through

[*] J. J. Richardson, Dr. H. Ejima, S. L. Lörcher, K. Liang, P. Senn, Dr. J. Cui, Prof. F. Caruso
Department of Chemical and Biomolecular Engineering
The University of Melbourne
Victoria 3010 (Australia)
E-mail: fcaruso@unimelb.edu.au

[**] F.C. acknowledges funding from the Australian Research Council under the Australian Laureate Fellowship scheme.

Supporting information for this article is available on the WWW under http://dx.doi.org/10.1002/anie.201302092.

centrifugation/wash cycles, the template particles can also be removed while still immobilized in the agarose gel (see below).

Layer buildup of PAH labeled with fluorescein isothiocyanate (FITC) and unlabeled PSS on 3.08 μm SiO_2 particles was confirmed through flow cytometry (Figure 2a). To prove that the fluorescence increase for each new bilayer was due to the newly loaded PAH, rather than residual PAH in the agarose, PAH labeled with rhodamine isothiocyanate (RITC) and AlexaFluor 647 (AF647) was used instead of PAH–FITC for the second and third polymer bilayers, respectively (Figure 2c). The resulting capsules exhibited fluorescence corresponding to each individual bilayer; this fluorescence confirmed that each subsequent layer of PAH had been adsorbed onto the particles. Similarly, PSS–RITC[10] was layered after PAH–FITC to show that PSS was incorporated into the films along with PAH (Figure 2d), whereas eight-layer controls of solely PAH or PSS did not produce capsules (data not shown). ζ-Potential measurements showed that the surface charge alternated between two values upon layering with PAH and PSS, although the ζ-potential was always negative (Figure 2b). The negative values are most likely due to the rearrangement of polymers upon heating, which is required for the collection of the particles from the agarose. Capsules prepared by the conventional LbL method (i.e., solution adsorption/centrifugation) also exhibited a negative ζ-potential after heating, regardless of the outer layer (see Figure S1 in the Supporting Information). Finally, we used attenuated total reflectance FTIR spectroscopy to show that capsules prepared by conventional LbL assembly and EPA have similar peaks, whereby the capsules assembled by EPA lack the peaks unique to agarose (see Figure S2 in the Supporting Information). For comparison, the use of the conventional LbL approach to deposit four PAH/PSS bilayers on micron-sized particles would typically take about 4 h, whereas the same number of layers can be deposited on a similar number of particles by EPA in approximately 2 h, as the need for manual washing steps is eliminated. For smaller particle templates (e.g., nanoparticles), EPA can offer time savings of up to 80% (depending on the particle templates and polymers used). Similar polymer amounts to those used in conventional LbL assembly are also used in EPA (see the Supporting Information).

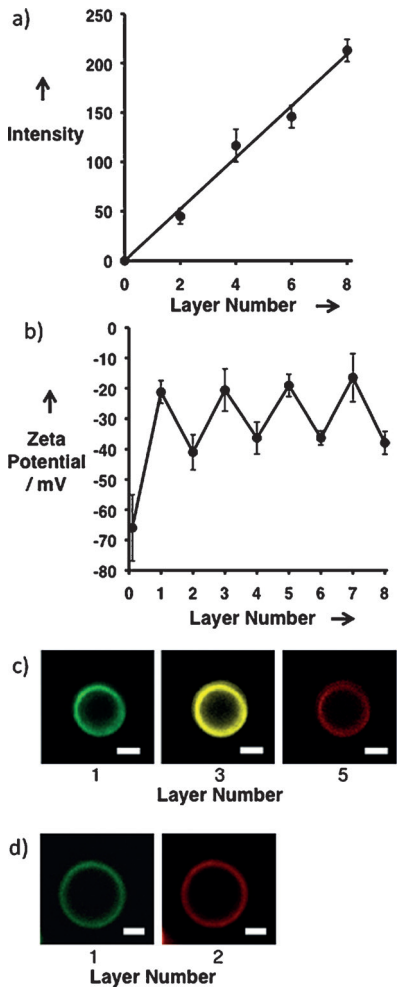

Figure 2. Buildup of PAH/PSS layers by EPA on SiO_2 particles with a diameter of 3.08 μm. a) Increase in fluorescence intensity and b) ζ-potential as a function of the number of layers. Odd layer numbers correspond to PAH deposition and even layer numbers to PSS deposition. c) Imaging of a single capsule with three different wavelengths: layer 1: PAH–FITC (green); layer 3: PAH–RITC (yellow); layer 5: PAH–AF647 (red). Scale bars: 2 μm. d) Imaging of a capsule with two different wavelengths: layer 1: PAH–FITC (green); layer 2: PSS–RITC (red). Scale bars: 1 μm.

We next investigated EPA onto smaller particles. Four bilayers of PAH/PSS were used to coat SiO_2 particles with diameters of 1.10 μm, 585 nm, and 35 nm. Spin columns were used to remove agarose and buffered HF from the samples prepared on the 35 nm particles. The resulting capsules were approximately the same size as the template particles, and the hollow nature of the capsules (observed as "darker rings") was visible by fluorescence microscopy for the largest three particle sizes studied (Figure 3a–c); however, super-resolution stochastic optical reconstruction microscopy (STORM)[11] was necessary to image the capsules produced from the 35 nm particles (Figure 3d). Folds were observed by transmission electron microscopy (TEM; Figure 3e–h) and scanning electron microscopy (SEM; Figure 3i–l) in the larger capsules. Atomic force microscopy (AFM) of the capsules yielded wall thicknesses of (22 ± 2) nm for both the 3.08 and 1.10 μm capsules (see Figure S3 in the Supporting Information). The average individual layer thickness of 2.7 nm is approximately twice that typically observed ((1.3 ± 0.3) nm) for PAH/PSS capsules assembled by the conventional LbL approach (solution adsorption/centrifugation).[12] Possible reasons for this difference are the different assembly conditions (e.g., electrolyte concentration and electric current).

The capsules prepared from particles of 35 nm in diameter were well below the resolution limit of a standard fluorescence microscope, and STORM was required to observe these capsules after postlabeling with AF647 (Figure 4a). By using a spherical aberrator, we were able to observe the hollow nature and size of the capsules in a 3D reconstruction (Figure 4b). In 2D, the individually detected fluorophores and Gaussian fitting further confirmed the hollow and approximately spherical structure of the capsules (Figure 4c).

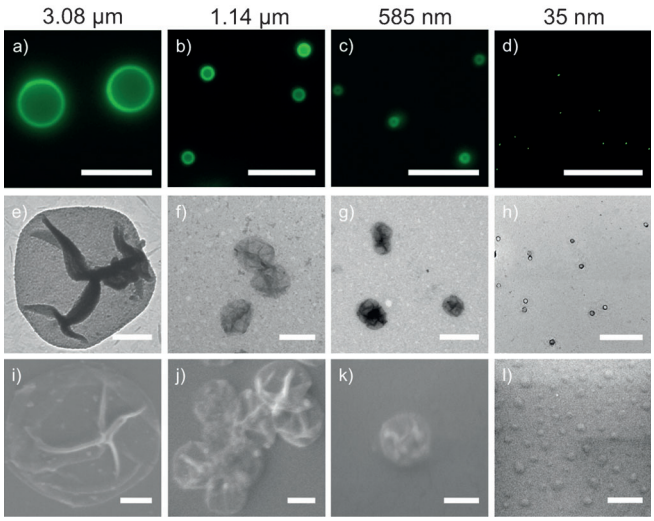

Figure 3. Microscopy images of four-bilayer PAH/PSS capsules obtained from PAH/PSS-coated SiO_2 particles of different size (3.08 μm, 1.10 μm, 585 nm, 35 nm) prepared by EPA. a–c) Fluorescence microscopy and d) STORM images of the capsules (scale bars: 5 μm). e–h) TEM images of the capsules (scale bars: 1 μm). i–l) SEM images of the capsules (scale bars: 500 nm).

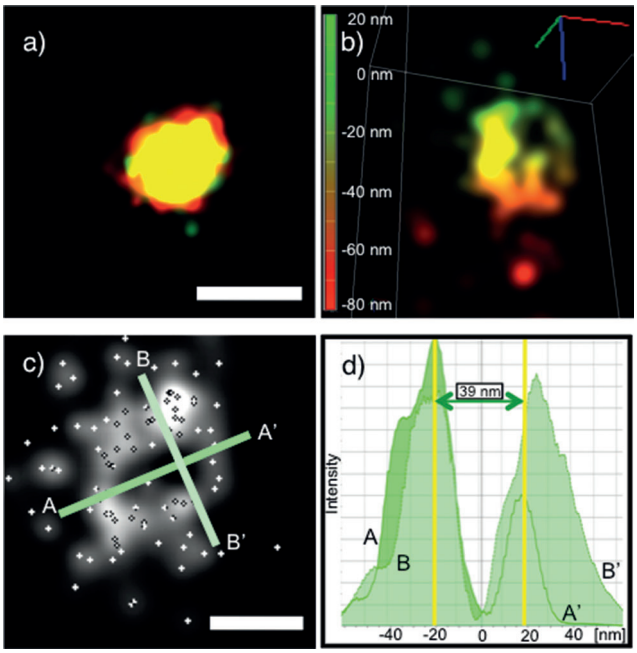

Figure 4. STORM imaging of a four-bilayer PAH/PSS capsule prepared from EPA of PAH/PSS on SiO_2 particles with a diameter of 35 nm. a) STORM image in which green corresponds to AF647 specifically activated by PAH–FITC, red corresponds to nonspecific AF647 activation, and yellow corresponds to the overlap of specific and nonspecific activation (scale bar: 100 nm). b) 3D STORM pseudocolor image of a capsule. The scale-bar colors and values correspond to the position in the *z* plane. c) Fluorescence profile created by Gaussian rendering on the basis of individually detected fluorophores (crosses; scale bar: 100 nm). d) Graphical representation of the 2D fluorescence intensity in (c) along the lines A–A′ and B–B′. The dark-green fluorescence profile across A–A′ is plotted behind the light-green fluorescence profile across B–B′.

The fluorescence profile of a hollow capsule showed a similar size to that found by TEM, and the distance between the fluorescence maxima was roughly equal to the particle size (Figure 4d; see also Figure S4 in the Supporting Information).

Having demonstrated the versatility of EPA with regard to particle size, we used other polymer combinations to assemble multilayers of different polymer compositions or stabilized through different interactions (i.e., hydrogen and covalent bonding). Similar to layering synthetic polyelectrolytes (PAH/PSS) (Figure 5a), the biopolymers poly-L-lysine (PLL) and poly-L-glutamic acid (PGA)[13] were layered through electrostatic association to yield robust capsules (Figure 5b). Particles were layered through covalent inter-

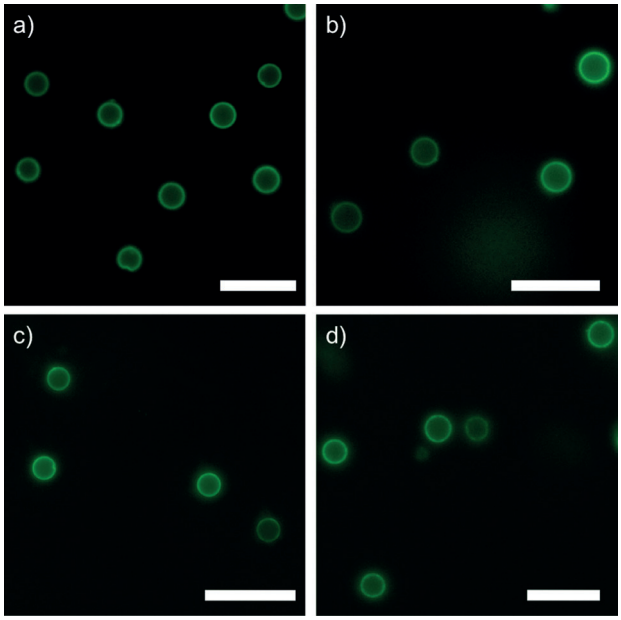

Figure 5. Fluorescence microscopy images of four-bilayer polymer capsules of different compositions prepared from polymer-coated 3.08 μm diameter SiO_2 particles synthesized by EPA: a) PAH–FITC/PSS capsules; b) PLL/PGA capsules postlabeled with AF488; c) PAH–FITC/GA capsules; d) PDPA–AF488/PMA capsules. Scale bars: 10 μm.

actions between the amines on PAH and the aldehyde groups of glutaraldehyde (GA)[4c] to also yield stable capsules after particle removal. Similar conditions to those used for PAH/PSS layering were used; however, GA was also loaded into the wells adjacent to the anode, and the electroendoosmotic effect (EEO)[8] was used to deposit the uncharged GA (Figure 5c). The hydrogen-bonding polymers poly(2-diisopropylaminoethyl methacrylate) (PDPA) and poly(methacrylic acid) (PMA)[4a] were layered similarly to PAH/PSS. After layering, the PDPA was cross-linked through azide–alkyne click chemistry to stabilize the films (Figure 5d).[4a] Layer buildup for the covalent-bonding (PAH/GA) and hydrogen-bonding polymers (PDPA/PMA) was monitored by flow cytometry (see Figure S5 in the Supporting Information). For the PDPA capsules, cross-linking was also performed in situ (in the agarose scaffold), and the template particles were removed while still immobilized in the agarose.

No discernible differences were observed if the template particles were cross-linked and/or removed in situ or ex situ (after recovery of the coated particles).

In summary, we have introduced an EPA method for the coating of particles with polymer multilayers and for the preparation of polymer nano- and microcapsules. Agarose acts as a natural, simple to use, thermally responsive, and safe immobilizing microfluidic hydrogel crucial for the preparation of core–shell particles and capsules by EPA. EPA is a versatile technique that holds promise as an efficient, potentially automatable method compatible with a diverse range of polymers and particle sizes. Charged biopolymers, covalently coupled polymers, and hydrogen-bonding polymers yielded stable capsules when layered; thus, this system preserves the versatility inherent to conventional LbL assembly with respect to the polymers that can be used. Importantly, layering on immobilized particles is not necessarily limited to electrophoretic deposition or the polymers, buffers, and particle-recovery method used in the reported experiments. The use of standard, inexpensive laboratory apparatus and materials opens up the potential for increased endeavors toward the development of LbL-assembled responsive drug- and gene-delivery systems generally, and also specifically in the sub-100 nm diameter size range.[14]

Received: March 13, 2013
Published online: May 9, 2013

Keywords: colloids · electrophoresis · nanomaterials · polymer capsules · super-resolution optical microscopy

[1] a) G.-D. Fu, G. L. Li, K. G. Neoh, E. T. Kang, *Prog. Polym. Sci.* **2011**, *36*, 127 – 167; b) K. Ariga, J. P. Hill, Q. Ji, *Phys. Chem. Chem. Phys.* **2007**, *9*, 2319 – 2349; c) S. Peyratout, L. Dahne, *Angew. Chem.* **2004**, *116*, 3850 – 3872; *Angew. Chem. Int. Ed.* **2004**, *43*, 3762 – 3783; d) G. K. Such, A. P. R. Johnston, F. Caruso, *Chem. Soc. Rev.* **2011**, *40*, 19 – 29; e) S. De Koker, R. Hoogenboom, B. G. De Geest, *Chem. Soc. Rev.* **2012**, *41*, 2867 – 2884; f) B. M. Wohl, J. F. J. Engbersen, *J. Controlled Release* **2012**, *158*, 2 – 14.

[2] a) A. Postma, Y. Yan, Y. Wang, A. N. Zelkin, E. Tjipto, F. Caruso, *Chem. Mater.* **2009**, *21*, 3042 – 3044; b) T. K. Mandal, M. S. Fleming, D. R. Walt, *Chem. Mater.* **2000**, *12*, 3481 – 3487; c) T. K. Goh, S. Guntari, C. J. Ochs, A. Blencowe, D. Mertz, L. A. Connal, G. K. Such, G. Q. Qiao, F. Caruso, *Small* **2011**, *7*, 2863 – 2867; d) G. L. Li, D. Wan, K. G. Neoh, E. T. Kang, *Macromolecules* **2010**, *43*, 10275 – 10282.

[3] a) E. Donath, G. B. Sukhorukov, F. Caruso, S. A. Davis, H. Möhwald, *Angew. Chem.* **1998**, *110*, 2323 – 2327; *Angew. Chem. Int. Ed.* **1998**, *37*, 2201 – 2205; b) F. Caruso, R. A. Caruso, H. Möhwald, *Science* **1998**, *282*, 1111 – 1114; c) *Colloids and Colloid Assemblies: Synthesis, Modification, Organization and Utilization of Colloid Particles* (Ed.: F. Caruso), Wiley-VCH, Weinheim, **2004**.

[4] a) K. Liang, G. K. Such, Z. Zhu, Y. Yan, H. Lomas, F. Caruso, *Adv. Mater.* **2011**, *23*, H273 – H277; b) Z. Y. Poon, D. S. Chang, X. Y. Zhao, P. T. Hammond, *ACS Nano* **2011**, *5*, 4284 – 4292; c) W. Tong, C. Gai, H. Möhwald, *Macromol. Rapid Commun.* **2006**, *27*, 2078 – 2083; d) D. I. Gittins, F. Caruso, *Adv. Mater.* **2000**, *12*, 1947 – 1949; e) D. I. Gittins, F. Caruso, *J. Phys. Chem. B* **2001**, *105*, 6846 – 6852; f) O. Shimoni, Y. Yan, Y. Wang, F. Caruso, *ACS Nano* **2013**, *7*, 522 – 530; g) G. Schneider, G. Decher, *Nano Lett.* **2004**, *4*, 1833 – 1839.

[5] A. Qi, P. Chan, J. Ho, A. Rajapaksa, J. Friend, L. Yeo, *ACS Nano* **2011**, *5*, 9583 – 9591.

[6] A. Voigt, H. Lichtenfeld, G. B. Sukhorukov, H. Zastrow, E. Donath, H. Baumler, H. Möhwald, *Ind. Eng. Chem. Res.* **1999**, *38*, 4037 – 4043.

[7] a) D. G. Shchukin, D. S. Kommireddy, Y. Zhao, T. Cui, G. B. Sukhorukov, Y. M. Lvov, *Adv. Mater.* **2004**, *16*, 389 – 393; b) C. Kantak, S. Yobas, T. Bansal, D. Trau, *Lab Chip* **2011**, *11*, 1030 – 1035; c) C. Priest, A. Quinn, A. Postma, A. N. Zelikin, J. Ralston, F. Caruso, *Lab Chip* **2008**, *8*, 2182 – 2187.

[8] S. Hjertén, *Biochim. Biophys. Acta* **1961**, *53*, 514 – 517.

[9] J. R. Brody, S. E. Kern, *Anal. Biochem.* **2004**, *333*, 1 – 13.

[10] A. P. R. Johnston, A. N. Zelikin, L. Lee, F. Caruso, *Anal. Chem.* **2006**, *78*, 5913 – 5919.

[11] M. J. Rust, M. Bates, X. Zhuang, *Nat. Methods* **2006**, *3*, 793 – 796.

[12] S. Leporatti, A. Voigt, R. Mitlohner, G. Sukhorukov, E. Donath, H. Möhwald, *Langmuir* **2000**, *16*, 4059 – 4063.

[13] D. T. Haynie, N. Palath, Y. Liu, B. Li, N. Pargaonkar, *Langmuir* **2005**, *21*, 1136 – 1138.

[14] H. Cabral, Y. Matsumoto, K. Mizuno, Q. Chen, M. Murakami, M. Kimura, Y. Terada, M. R. Kano, K. Miyazono, M. Uesaka, N. Nishiyama, K. Kataoka, *Nat. Nanotechnol.* **2011**, *6*, 815 – 823.

